

# Superconductivity in the Chalcogens up to Multimegabar Pressures

Eugene Gregoryanz<sup>1</sup>, Viktor V. Struzhkin<sup>1</sup>, Russell J. Hemley<sup>1</sup>, Mikhail I. Erements<sup>1</sup>,  
Ho-kwang Mao<sup>1</sup> and Yuri A. Timofeev<sup>2</sup>

<sup>1</sup>*Geophysical Laboratory and Center for High Pressure Research, Carnegie Institution of Washington,  
5251 Broad Branch Road NW, Washington D.C. 20015 U.S.A*

<sup>2</sup>*Institute for High Pressure Physics, Russian Academy of Science,  
142092 Troitsk, Moscow Region, Russia*

Highly sensitive magnetic susceptibility techniques were used to measure the superconducting transition temperatures in S up to 231( $\pm 5$ ) GPa. S transforms to a superconductor with  $T_c$  of 10 K and has a discontinuity in  $T_c$  dependence at 160 GPa corresponding to bco to  $\beta$ -Po phase transition. Above this pressure  $T_c$  in S has a maximum reaching about 17.3( $\pm 0.5$ ) K at 200 GPa and then slowly decreases with pressure to 15 K at 230 GPa. This trend in the pressure dependence parallels the behavior of the heavier members Se and Te. Superconductivity in Se was also observed from 15 to 25 GPa with  $T_c$  changing from 4 to 6 K and above 150 GPa with  $T_c$  of 8 K. Similarities in the  $T_c$  dependences for S, Se, and Te, and the implications for oxygen are discussed.

## I. INTRODUCTION

Comparative study of the high-pressure behavior of groups of elements (i.e. with identical valences) provides detailed insight into the effects of compression on electronic structure and its control of physical properties. The chalcogen elements, or members of group VIa, exhibit a variety of phases as a function of pressures and temperatures and exhibit a broad range of interesting physical properties.<sup>1</sup> The lighter members of the family form molecular crystals. The first is oxygen, which forms a diatomic molecular crystal and persists in a variety of molecular phases to at least 100 GPa.<sup>2</sup> It also has peculiar magnetic interactions, being the only magnetic insulator among elements.<sup>1</sup> At these higher pressures, however, oxygen not only becomes metallic<sup>3</sup> but is also superconducting<sup>4</sup> above 95 GPa. Theoretical calculations predict that the high-pressure  $\zeta$ -O<sub>2</sub> phase above 96 GPa is a molecular metal,<sup>5</sup> while unambiguous experimental evidence of its molecular character is still not available. Sulfur has one of the most complex diagrams of the elements.<sup>1</sup> Under ambient conditions, sulfur is molecular and consists of S<sub>8</sub> species that form rings in the crystalline state. Under pressure, sulfur undergoes a series of both stable and metastable phase transitions up to  $\sim 90$  GPa, finally becoming metallic at higher pressures.<sup>6</sup>

Under pressure the heavier group VIa elements (below oxygen) undergo structural phase transitions involving non-molecular or extended structures and become metallic (with the exception of Po which is a metal at room pressure). Sulfur, selenium, and tellurium follow similar trends in the sequence of observed crystal structures. At comparatively low pressures, they crystallize in base-centered orthorhombic (bco) structures, which are metallic and superconducting. The situation is not as simple at pressures below the stability range of the bco phase. The sequence of phase transitions in Se below 30 GPa depends on the starting phase of the material.<sup>7</sup> An unidentified metallic phase was found in selenium (starting from pressures about 13 GPa) which was found to

be superconducting with  $T_c=5.2$  K at 17 GPa.<sup>7</sup> Sulfur also has an unidentified phase below 90 GPa,<sup>8</sup> which is however, semiconducting.<sup>6</sup> On further compression in the bco phase, S, Se and Te transform to the rhombohedral  $\beta$ -Po structure. If compressed to even higher pressures at room temperature, Te and Se transform to the body-centered (bcc) structure at 27 GPa (Ref. 9) and 140 GPa (Ref. 10), respectively.

The high-pressure structural and electronic properties of these elements have been the subject of a variety of theoretical studies. Pseudopotential total energy calculations<sup>11</sup> have been performed for three high-pressure phases of S. They suggested that S should transform from the  $\beta$ -Po to the bcc phase at 545 GPa which would have a strong electron-phonon coupling leading to a superconducting transition temperature of 15 K. More recent first-principles calculations<sup>12</sup> predict that compressed S favors the simple cubic structure over a wide range of pressures from 280 GPa to 540 GPa before transforming to a bcc phase. The later work also showed that upon entering the simple cubic structure, the average phonon frequency  $\langle \omega \rangle$  increases substantially, leading to a smaller  $\lambda$  and thus smaller  $T_c$ . It was predicted that  $T_c$  would drop below 10 K upon entering the proposed simple cubic phase.<sup>12</sup>

Recent experimental studies<sup>13,14</sup> showed that sulfur becomes metallic and superconducting at 93 GPa (with  $T_c=10.1$  K) and when pressurized above 160 GPa in  $\beta$ -Po phase it has one of the highest known transition temperatures among the elements (17 K). Here we present a comparative study of pressure-induced superconductivity in the chalcogens up to multimegabar ( $> 200$  GPa) pressures. We extended the measurements of superconductivity in S by magnetic susceptibility up to 231( $\pm 5$ ) GPa, which is the record pressure for such an experiment. We also present results for  $T_c$  in Se by direct resistance measurements from 15 to 25 GPa and by magnetic susceptibility up to 180( $\pm 5$ ) GPa in the bcc phase.

## II. EXPERIMENTAL DETAILS

We performed the measurements of  $T_c$  of S and Se using an improved extension of a highly sensitive diamond-anvil cell magnetic susceptibility technique described previously.<sup>15</sup> This technique is based on the quenching of superconductivity and suppression of the Meisner effect in the sample by an external magnetic field. The susceptibility of the metallic diamagnetic parts of the diamond cell is essentially independent of the external field. Applying a magnetic field to the diamond cell (and sample) will therefore change the signal coming from the sample while the background arising from the surrounding diamagnetic parts will be nearly constant. The measurements are done with four coils (shown in Fig. 1). Two small coils consist of a signal coil, which is wound around the sample (1) and a compensating coil (2) connected in opposition. The excitation coil (3) encompasses both the signal and compensating coils. The alternating high-frequency magnetic field at the signal coil is created by the excitation coil fed from the high-frequency generator. The alternating magnetic field excites electromotive forces in the signal coil. The fourth coil (4) placed around the diamond cell is used to destroy the superconductivity in the sample near the superconducting transition by application of a low-frequency ( $f=20$  Hz) magnetic field with an amplitude of several tens of Oersteds. This leads to a change in magnetic susceptibility of the sample from -1 to 0 twice in a given period and produces a modulation of the signal amplitude in the signal coil with a frequency  $2f$ . The lock-in technique is used to record this signal as a function of temperature. The technique sensitivity was improved recently by using higher modulation frequency in the excitation-pickup coil set up.<sup>16</sup>

Samples of 99.9995% purity S were loaded in Mao-Bell cells<sup>17</sup> made from Be-Cu and modified for measurements down to liquid helium temperatures. The gaskets made from nonmagnetic Ni-Cr alloy were used together with tungsten inserts to confine the sample and no pressure transmitting medium was used. The gasket and insert may be responsible for the temperature dependent background seen in the raw temperature scans (e.g., Fig. 2). To reach pressures above 200 GPa we used beveled diamonds with 50  $\mu\text{m}$  flats and 300  $\mu\text{m}$  outer culets. The initial sample size was  $\sim 35$   $\mu\text{m}$  in diameter and  $\sim 10$   $\mu\text{m}$  thickness. Pressures were measured by the ruby fluorescence technique (quasihydrostatic scale)<sup>18</sup> using  $\text{Ar}^+$  and Ti-sapphire laser excitation *in situ* at low temperatures.

For Se, we used direct conductivity measurements of sample resistance up to 35 GPa.<sup>19</sup> Four electrical leads formed from platinum foil allowed four-electrode measurements of the resistance. To insulate the electrodes from the metallic gasket, an insulating layer made from the mixture of cubic boron nitride powder and epoxy was used. The superconducting transition was detected by direct resistance measurements and by using a modulating technique similar to that used in the susceptibility exper-

iments. At higher pressures (up to 180 GPa) we used the magnetic susceptibility technique described above. The configurations of the cell, diamonds, gasket and ruby fluorescence measurement technique were identical to that used in the S experiments.

## III. RESULTS AND DISCUSSION

### A. Superconductivity in S to 230 GPa

Several runs were made with decreasing sample sizes and diamond culet dimensions to successively higher pressures. Measurements are made as a function of temperature. Representative results are shown in Figs. 2-4. No superconductivity was detected up to approximately 90 GPa. At 93 GPa, however, a peak characteristic of the superconducting transition to the superconducting state was observed.<sup>15</sup>  $T_c$  is identified as the temperature where the signal goes to zero on the high temperature side (e.g., Fig.4), which is the point at which magnetic flux completely enters the sample.<sup>15</sup> Two peaks are clearly seen at  $\sim 10$ -12 K and  $\sim 17$  K. The second broad peak at lower temperatures arises from the sample outside of the flat culet, where pressure is considerably lower than in the middle of the culet. At pressures over 190 GPa the peak at 17 K becomes visibly split. This splitting is artificial and only reflects the fact that the signal amplitude has increased substantially with respect to the background.

The background signal in our measurements appeared to be ferromagnetic, as its phase is approximately opposite to that of the signal from the sample (diamagnetic) (see Fig. 2). Because the background signal changes smoothly with temperature, we can separate the signal from the background by the simple procedure illustrated in Fig. 3. We measure amplitude and phase of a sum of signal and background with the lock-in technique. The signal changes very abruptly in the vicinity of the superconducting transition, allowing us to see these changes both in amplitude and phase (Fig. 3). It is straightforward to interpolate the background in the range of the superconducting transition with a smooth polynomial function. The total signal can be represented as the complex variable  $\mathbf{U} = A_S e^{i\phi_S}$ , and the interpolated background as  $\mathbf{B} = A_B e^{i\phi_B}$ ; our signal is then  $\mathbf{S} = A_S e^{i\phi_S} = \mathbf{U} - \mathbf{B}$  (the difference of two complex variables).

The signal with background subtracted is shown in Fig. 4. As in previous work,<sup>14</sup> we observed the appearance of a  $T_c$  signal at  $\sim 93$  GPa at 10 K.  $T_c$  gradually increases and upon entering the  $\beta$ -Po phase at 165 GPa it jumps to 17.0( $\pm 0.5$ ) K. For the next 35 GPa, it still slowly increases, reaching a weak maximum of 17.3( $\pm 0.5$ ) K at 180-200 GPa; it then decreases on further compression, dropping to 15 K at 231 GPa.

## B. Superconductivity in Se to 180 GPa

Two sets of experiments were performed on Se. In the first experiment, we used 99.999% pure amorphous Se as the starting material with NaCl as pressure transmitting medium. Raman spectra showed that Se crystallized at around 11 GPa.<sup>21</sup> A measurable  $T_c$  signal appeared at  $\sim 25$  GPa at 5.8 K, in agreement with previous studies.<sup>22</sup> Figure 5 shows the dependence of resistance and its modulations by the magnetic field as a function of temperature. In both cases, the onset of the superconducting transition in the sample is clearly seen. After reaching 35 GPa, the pressure was released. The  $T_c$  signal was observable down to 18 GPa and decreased with releasing pressure.

In the second set of experiments amorphous Se was pressurized up to 180 GPa and  $T_c$  was measured by susceptibility technique. Currently, it is difficult to measure  $T_c$  signals of  $\sim 30 \mu\text{m}$  in diameter samples with this technique if the temperature of superconducting transition is below 4 K due to a developing background signal which is probably related to paramagnetic signal from the gasket (tungsten inset and Ni-Cr-Al alloy gasket material). We were able to detect the superconducting signal in the bcc phase from 140 to 180 GPa. On decompression below 130 GPa, the measurable signal disappeared.

## C. Comparison of $T_c$ among the chalcogens

The pressure dependences of  $T_c$  in the group VIA elements are shown in Fig. 6, together with the observed transition pressures between the phases. It should be noted that these boundaries were determined by x-ray diffraction at room temperature while the observations of superconductivity were done at temperatures ranging from 2 to 18 K. It may be assumed that the phase boundaries at low temperatures (if any) would be shifted in pressure. The observed structures are illustrated in Fig. 7.

Tellurium becomes superconducting in the monoclinic phase at  $\sim 4$  GPa. As shown in Fig. 6c,  $T_c$  rises linearly with pressure in this phase upon transforming to the bco structure, it levels off and starts to decrease, passing through the field of stability of the  $\beta$ -Po phase.  $T_c$  then jumps by almost factor of three and starts to come down again. This jump in  $T_c$  happens at 35 GPa while room temperature phase transition to bcc phase happens at 27 GPa.

Under ambient conditions, Se can be found in trigonal, monoclinic or amorphous forms. Akahama *et al.*<sup>7</sup> showed that monoclinic and trigonal Se become metallic at 12 and 23 GPa respectively. Under pressure amorphous Se crystallizes in a trigonal structure and becomes metallic at 12 GPa. It was shown<sup>7</sup> that if  $\alpha$ -monoclinic Se used as the starting material, it transforms at 12 GPa to an unidentified metallic phase which is superconducting at

17 GPa but no pressure dependence of  $T_c$  was given. Figure 6b shows our results for Se combined with the results of Ref.<sup>22</sup> The trend in the  $T_c$  dependence for Se is remarkably similar to that of Te, although unlike the latter, Se becomes metallic and superconducting in an unidentified phase from 14 to 23 GPa. The structural sequence is identical to that of Te starting from 23 GPa where Se enters the monoclinic phase. Unlike the situation for Te,  $T_c$  within this phase changes little with pressure. When Se is compressed further, the abrupt decrease in  $T_c$  starts at 33 GPa which can be attributed to the transition to the bco phase, which happens at 27 GPa at room temperature. There are no experimental measurements of  $T_c$  for Se from 60 to 150 GPa, but theoretical calculations<sup>24</sup> predict a decrease of  $T_c$  in the  $\beta$ -Po phase, followed by an increase to much higher values around 140 GPa where Se transforms to the bcc structure at 300 K. The values of  $T_c$  in Se at 150-170 GPa measured here are very close to those calculated in Ref. 24.

The structures of the semiconducting phases of S below the 90 GPa transition is not known. It becomes metallic and superconducting in the bco phase. Unlike the behavior of Se and Te,  $T_c$  in this phase of S increases with pressure and jumps abruptly upon entering the  $\beta$ -Po-type phase (Fig. 6a). In the  $\beta$ -Po phase,  $T_c$  slowly decreases with further compression. This decrease is consistent with the theoretical calculations of Rudin *et al.*<sup>12</sup>, which predicted a decrease in the electron-phonon coupling parameter  $\lambda$  as the sc phase is approached.<sup>12</sup>

It can be clearly seen from the behavior of the  $T_c$  for the three elements that the transition temperatures cannot be simply explained by the existence of phase transitions and similar values for electron-phonon coupling alone. On the other hand, the similar trends are broadly consistent with changes towards higher symmetry structures (transformation of layered phases to the close packed structures at the highest pressures) with weakening of the directional covalent bonding, as we now discuss.

Mössbauer studies of Te showed a decrease in the quadrupole splitting with pressure that was ascribed to strengthening interactions between the neighboring chains and weakening of the covalent bonds within the chain.<sup>27</sup> The splitting disappeared when Te was pressurized into the bcc phase where no covalent bonding is present. Thus we assume that the continuous weakening of the covalent bonds with increasing pressure is due to increasing screening by free carriers due to increasing density of states at the Fermi level.

To analyse the possible  $T_c$  increase in the lower pressure phases of the chalcogens due to the change in phonon spectra, we estimated  $T_c$  in the lower symmetry "layered" structures (i.e monoclinic, bco) using the Allen-Dynes formula<sup>25</sup> with literature values of  $\lambda$  (electron-phonon coupling constant) and  $\mu^*$  (effective Coulomb repulsion potential). We assumed  $\mu^*=0.1$  and varied  $\lambda$ . The values of  $\langle \omega_{log} \rangle$  and  $\langle \omega^2 \rangle$ , the averages of the phonon frequencies weighted to represent the

strength of the electron-phonon coupling, were estimated with the phonon density of states shown in Fig. 8. The density of states was assumed to have two cutoff Debye frequencies with values typical for Se and Te corresponding to intralayer bond-stretching and inter-layer vibrations. In our estimates of  $T_c$  versus pressure, the lower energy peak which we attributed to interlayer vibrations was allowed to move towards higher energies with pressure increase while the higher energy peak representing intralayer bond-stretching modes was assumed to be pressure-independent. The values of  $T_c$  obtained in these calculations are within the range of the experimentally observed  $T_c$  for Se and Te in their monoclinic and bco structures. However,  $T_c$  is virtually independent of phonon spectra but instead depends on  $\lambda$ . From experimental data,  $\lambda$  increases with pressure, meaning that  $N(E_F) < I^2 >$  increases faster than  $M < \omega^2 >$  (which does not change substantially in our simplified model), where  $\lambda = \frac{N(E_F) < I^2 >}{M < \omega^2 >}$ , according to McMillan<sup>26</sup>. Here  $N(E_F) < I^2 >$  is the Hopfield parameter, which is generally assumed to be inversely proportional to volume in simple s-p metals<sup>26</sup>. Thus, the increase in  $T_c$  observed in the monoclinic phase of Te and the unidentified phase of Se where covalent bonding is still significant is most probably governed by the increase in Hopfield parameter with pressure. Sulfur has increasing  $T_c$  in its bco phase where covalent bonding is still present.

The bco  $\rightarrow$   $\beta$ -Po  $\rightarrow$  bcc structural sequence may also be possible for oxygen, although the stability of its diatomic state appears to extend to very high pressures ( $> 100$  GPa<sup>28</sup>). It remains to be determined at what pressures the oxygen molecules dissociate (at low temperature), and what crystal structures would form. The additional complication with oxygen is its magnetic properties, which could play important role in determining  $T_c$ . If oxygen follows a similar structural trend in its nonmolecular state, a similar  $T_c$  dependence might be expected. Recent calculations<sup>29</sup> suggest that could be in 1 TPa range.

#### D. Conclusions

We have measured  $T_c$  of S up to 231 GPa, a record pressure for both superconductivity and magnetic susceptibility techniques. The value of  $T_c$  at the highest pressures (15 K above 200 GPa, decreasing from 17 K at 160 GPa) in accord with the original theoretical predictions for the hypothetical bcc phase<sup>11</sup> and more recent calculations for the  $\beta$ -Po structure<sup>12</sup>. The superconducting behavior of Se was observed in an unidentified phase from 14 to 20 GPa. The  $T_c$  for Se is also in very good agreement with recent first-principles calculations<sup>24</sup> (assuming  $\beta$ -Po, bcc, fcc structures). The data obtained in the present work, previously published experimental data, and recent theoretical calculations for the chalcogens allow us to conclude that at lower pressures  $T_c$  is

controlled at least in part by changes in covalent bonding. In higher pressures the bcc phases of these materials, the behavior of  $T_c$  resembles normal  $p$  metals and decreases with pressure.

#### E. Acknowledgements

We thank A. Liu for sharing results on Se prior to publication and S. Rudin and P. Dera for helpful discussions. This work was supported by the National Science Foundation.

- 
- <sup>1</sup> D.A. Young, *Phase Diagrams of the Elements*, Univ. of California Press, (Oxford, England 1991).
  - <sup>2</sup> M. Nicol and K. Syassen, Phys. Rev. B **28**, 1201 (1983); R. Meier and R. Helmholdt, Phys. Rev. B **29**, 1201 (1984); F. Gorelli *et al.*, Phys. Rev. Lett. **83**, 4093 (1999); F. Gorelli *et al.*, Phys. Rev. B **60**, 6179 (1999); R. Bini *et al.*, J. Chem. Phys. **112**, 8522 (2000).
  - <sup>3</sup> S. Desgreniers, Y. K. Vohra and A. L. Ruoff, J. Phys. Chem. **94**, 1117 (1990).
  - <sup>4</sup> K. Shimizu *et al.*, Nature **393**, 1333 (1998).
  - <sup>5</sup> S. Serra, G. Chiarotti, S. Scandolo and E. Tosatti, Phys. Rev. Lett. **80**, 5160 (1998).
  - <sup>6</sup> H. Luo, S. Desgreniers, Y.K. Vohra and A. Ruoff, Phys. Rev. Lett. **67**, 2998 (1991).
  - <sup>7</sup> Y. Akahama, M. Kobayashi and H. Kawamura, Phys. Rev. B **56**, 5027 (1997).
  - <sup>8</sup> Y. Akahama, M. Kobayashi and H. Kawamura, Phys. Rev. B **48**, 6862 (1993).
  - <sup>9</sup> G. Parthasarathy and W. B. Holzapfel, Phys. Rev. B **37**, 8499 (1988).
  - <sup>10</sup> Y. Akahama, M. Kobayashi and H. Kawamura, Phys. Rev. B **47**, 20 (1993).
  - <sup>11</sup> O. Zakharov and M. L. Cohen, Phys. Rev. B **52**, 12572 (1995).
  - <sup>12</sup> S. Rudin and A. Liu, Phys. Rev. Lett. **83**, 3049 (1999).
  - <sup>13</sup> S. Kometani *et al.*, J. Phys. Soc. Jap., **66**, 2564 (1997).
  - <sup>14</sup> V.V. Struzhkin, R.J. Hemley, H.K. Mao and Yu.A. Timofeev, Nature **390**, 382 (1997).
  - <sup>15</sup> Yu. A. Timofeev, Pribory i Technika Eksperimenta (in Russian), **5**, 190 (1992).
  - <sup>16</sup> Yu. A. Timofeev, V.V. Struzhkin, E. Gregoryanz, H. K. Mao, R. J. Hemley, Rev. Sci. Instr. (in press).
  - <sup>17</sup> H. K. Mao, R. J. Hemley and A. L. Mao *High-Pressure Science and Technology-1993* (eds S. Schmidt *et al.* 1613-1616 (American Institute of Physics, New York, 1994).
  - <sup>18</sup> H. K. Mao, J. Xu, P. M. Bell, J. Geophys. Res. **91**, 4673 (1986).
  - <sup>19</sup> M. Eremets *et al.*, Phys. Rev. Lett. **85**, 2797 (2000).
  - <sup>20</sup> J. Xu, H. K. Mao and P. M. Bell, High Temp. - High Press. **16**, 495 (1984).
  - <sup>21</sup> A. K. Bandyopadhyay and L. C. Ming, Phys. Rev. B **54**, 12049 (1996).

- <sup>22</sup> Y. Akahama *et al.*, Solid State Commun. **84**, 803 (1992).  
<sup>23</sup> I.V. Berman, Zh.I. Binzarov and P. Kurkin, Sov. Solid State, **14**, 2192 (1973).  
<sup>24</sup> S. Rudin, A. Liu, J. Freericks and A. Quandt arXiv:cond-mat/0011449 v. 1 (Nov. 2000).  
<sup>25</sup> P.B. Allen and R.C. Dynes, Phys. Rev. B, **12**, 905 (1975).  
<sup>26</sup> W. L. McMillan, Phys. Rev. **167**, 331 (1968).  
<sup>27</sup> P. Vulliet and J.P. Sanchez, Phys. Rev. B, **58**, 171 (1998).  
<sup>28</sup> P. Loubere, private communications.  
<sup>29</sup> M. Otani, K. Yamaguchi, H. Miyagi and N. Suzuki, Rev. High Press. Sci. Tech. **7** 178 (1998).

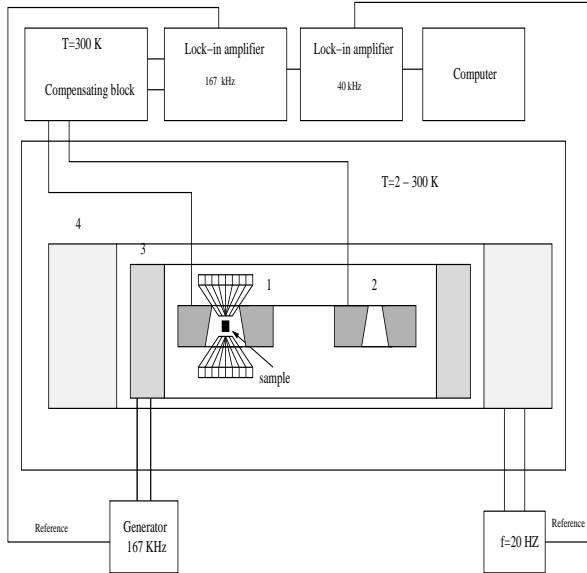


FIG. 1. Schematic diagram of the diamond anvil cell magnetic susceptibility technique.

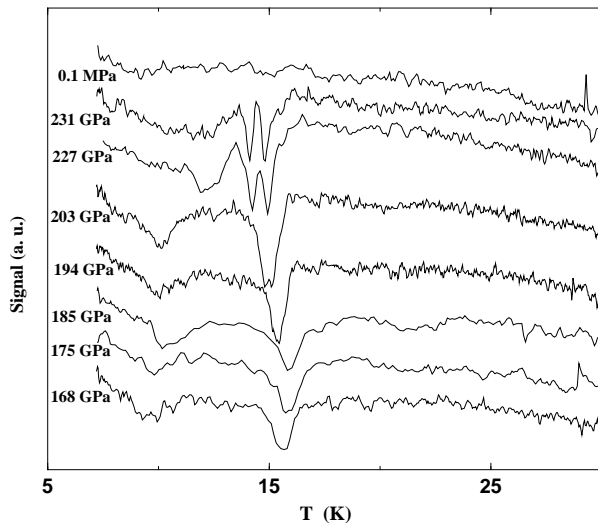


FIG. 2. Typical signal recorded for S during low-temperature scans. The top scan (background) was measured after the high-pressure run.

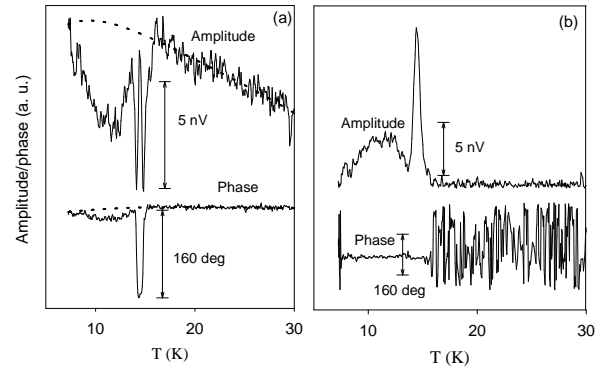


FIG. 3. Procedure for background subtraction. (a) Total signal can be represented as the complex variable  $U = A_{S+B}e^{i\phi_{S+B}}$  and the interpolated background is just  $B = A_B e^{i\phi_B}$ . (b) The signal is equal to  $S = U - B$

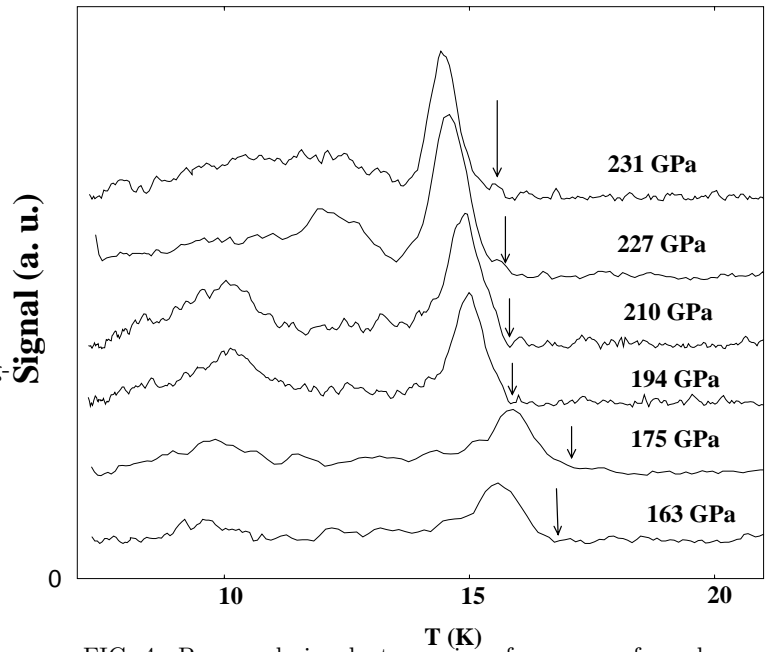


FIG. 4. Processed signal at a series of pressures for sulfur. The wide peak at lower temperatures is from the sample outside of the culet.

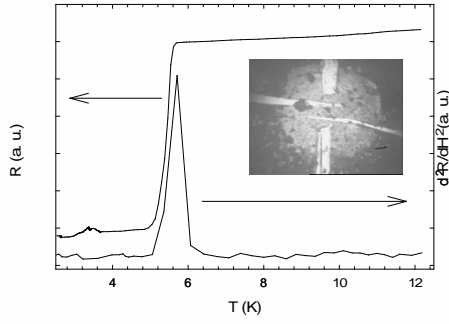


FIG. 5. Temperature dependence of resistance and resistance modulated by the magnetic field for Se. Inset: micrograph of the 4-probe electrodes arrangement used in these measurements.

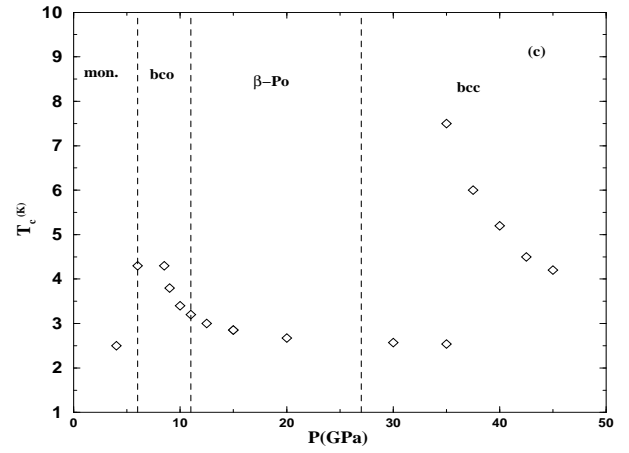
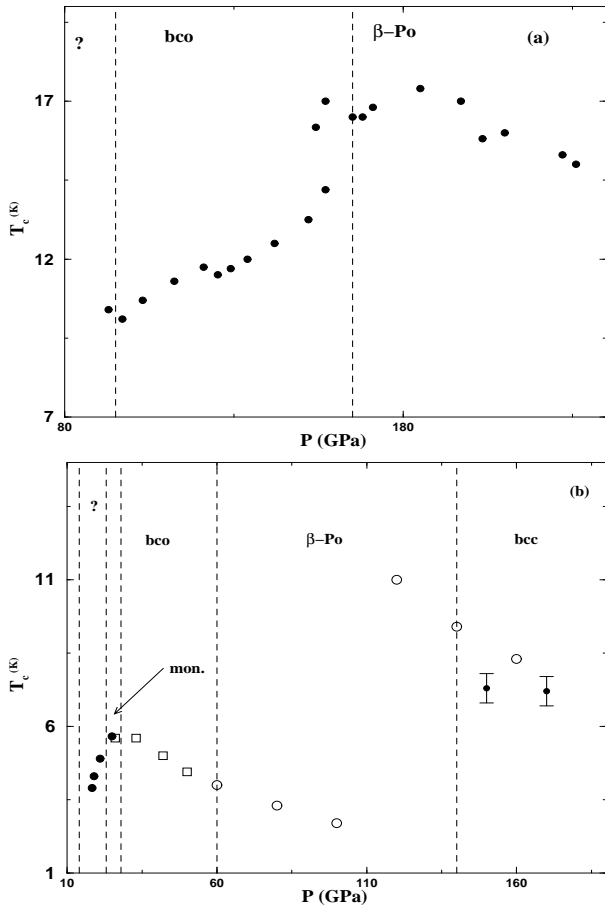
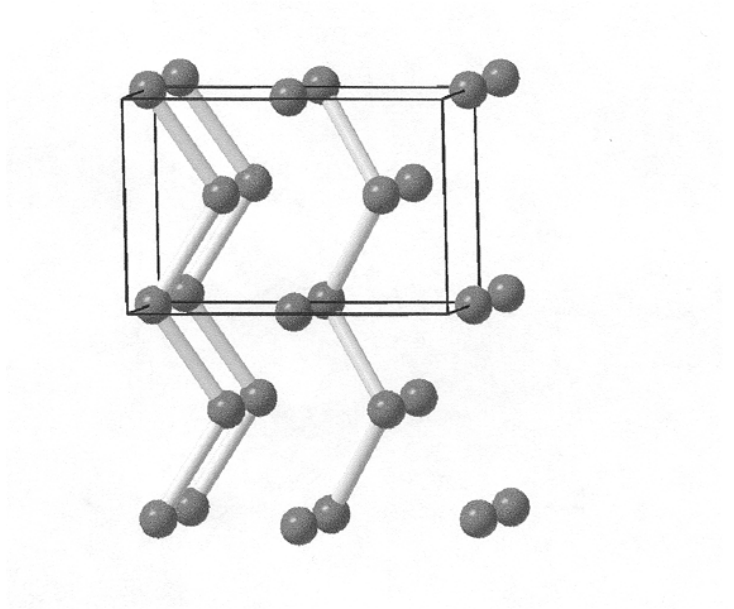


FIG. 6. Temperature dependences of  $T_c(P)$  in (a) S, (b) Se, and (c) Te. The experimental dependences of  $T_c(P)$  for Se and Te shown as open diamonds are from Refs. [ 22,23]. The theoretical calculation for Se shown in (b) with open circles are from Ref. [ 24]. The dashed lines are the phase boundaries measured at room temperature by x-ray diffraction.

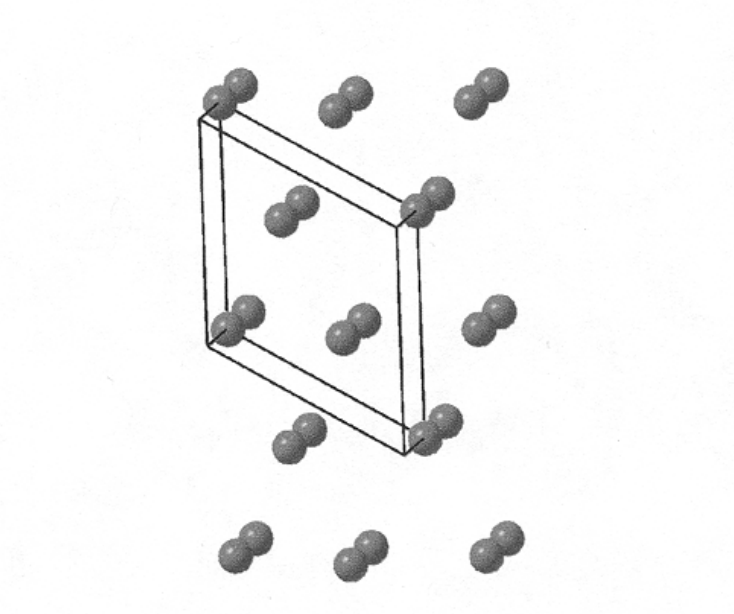
i



a)



b)



c)

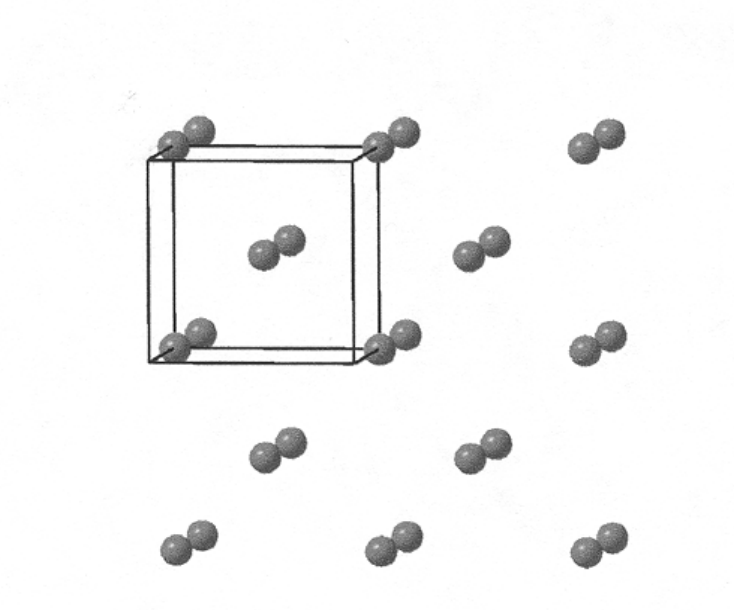


FIG. 7. Comparison between the (a) bco, (b)  $\beta$ -Po, and (c) bcc structures.

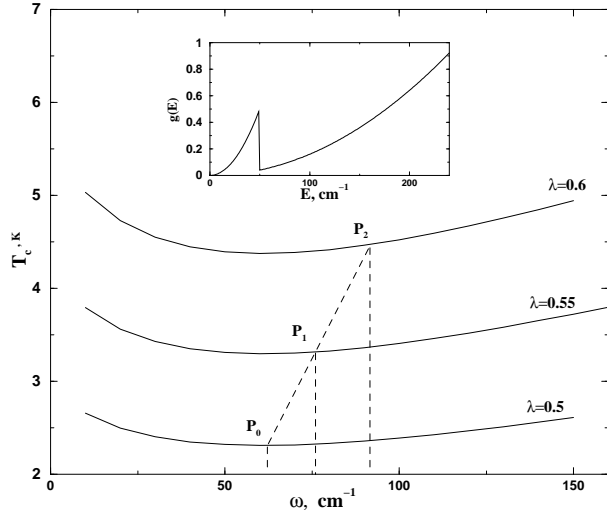


FIG. 8.  $T_c$  as a function of the pressure dependent Debye frequency. Inset: the density of states used to calculate  $\langle \omega_{log} \rangle$ . The dashed line shows the increase in  $T_c$  corresponding to the increase in Debye frequency and  $\lambda$ , which was varied from 0.5 to 0.6. The increase in frequency corresponds to the increase in pressure by  $\sim 20\%$ - $30\%$ .